

Aerosols and clouds in the upper troposphere–lower stratosphere region detected by GOMOS and ACE: Intercomparison and analysis of the years 2004 and 2005

J. Dodion ^{a,*}, D. Fussen ^a, F. Vanhellemont ^a, C. Bingen ^a, N. Mateshvili ^a, K. Gilbert ^b, R. Skelton ^b, D. Turnbull ^b, S.D. McLeod ^b, C.D. Boone ^b, K.A. Walker ^b, P.F. Bernath ^b

^a Belgian Institute for Space Aeronomy, Ringlaan 3, B-1180, Brussels, Belgium

^b Department of Chemistry, University of Waterloo, Waterloo, Ont., Canada

Received 19 January 2007; received in revised form 1 August 2007; accepted 4 September 2007

Abstract

Satellite-based limb occultation measurements are well suited for the detection and mapping of polar stratospheric clouds (PSCs) and cirrus clouds. PSCs are of fundamental importance for the formation of the Antarctic ozone hole that occurs every year since the early 1980s in Southern Hemisphere spring. Despite progress in the observation, modeling and understanding of PSCs in recent years, there are still important questions which remain to be resolved, e.g. PSC microphysics, composition, formation mechanisms and long-term changes in occurrence. In addition, it has recently become clear that cirrus clouds significantly affect the global energy balance and climate, due to their influence on atmospheric thermal structure.

Since 2002, two major space missions using the occultation method have been put into orbit: the European stellar occultation spectrometer GOMOS on board ENVISAT and the Canadian solar occultation instruments ACE-FTS/MAESTRO on board SCISAT-I.

PSCs and cirrus clouds are detected both by ACE and GOMOS. The results of an intercomparison between retrieved aerosol extinction, PSCs and cirrus clouds are the subject of this paper. The cloud data are also used to examine the evolution of PSCs over the Antarctic vortex and the latitudinal variation of tropical cirrus for the years 2004 and 2005.

© 2007 COSPAR. Published by Elsevier Ltd. All rights reserved.

Keywords: Aerosols; PSCs; Cirrus clouds; Remote sensing

1. Introduction

Since its discovery (Junge et al., 1961), the stratospheric aerosol layer has gained increasing attention because of its role in a number of atmospheric phenomena. Owing to their interaction with UV, visible and infrared radiation, aerosols are likely to play a significant role in the Earth's radiative budget and climate (Dutton and Christy, 1992). Explosive volcanic eruptions emit sulfur species into the stratosphere, mainly in the form of SO₂. These sulfur species react with OH and H₂O to form H₂SO₄ on a timescale

of weeks, and the resulting H₂SO₄/H₂O aerosol droplets produce the dominant radiative effect from volcanic eruptions. Once injected into the stratosphere, the aerosol particles are rapidly advected around the globe. The last volcanic eruption of this strength, Mount Pinatubo in the Philippines, occurred in 1991. Since then, due to slow sedimentation, the aerosol abundance has gradually decreased to the present day level, the lowest in decades. Nevertheless, the absorption/scattering efficiency of aerosols is such that they still show their imprint in a wide range of optical measurements.

Polar stratospheric clouds are of fundamental importance for the formation of the Antarctic ozone hole (Farman et al., 1985) that occurs every year since the early

* Corresponding author. Tel.: +32 23730378; fax: +32 23748423.

E-mail address: jan.dodion@bira-iasb.be (J. Dodion).

1980s in Southern Hemisphere spring. Enhanced ozone depletion is linked to heterogeneous chlorine chemistry that occurs on the surfaces of PSCs at cold temperatures (e.g. Molina et al., 1987; Solomon, 1999).

In addition, it has recently become clear that cirrus clouds significantly affect the global energy balance and climate, due to their influence on atmospheric thermal structure. Several studies (e.g. Randall et al., 1989; Ramaswamy and Ramanathan, 1989; Liu et al., 2003a,b) point out that cirrus clouds are likely to have great impact on the radiation and hence the intensity of the general large-scale circulation in the tropics. Cirrus generally occur below the spontaneous freezing temperature of water, and are therefore populated by ice crystals, which usually exist in some cylindrical form such as hexagonal columns. In situ measurements and model simulations show that cirrus are populated by crystals with lengths between about 10 and 500 μm at concentrations from roughly 0.01 to 100 cm^{-3} (Jensen et al., 1994). Cirrus clouds are globally distributed at all latitudes over land or sea at any season of the year. They undergo continuous changes in area coverage, thickness, texture, and position. Tropical cirrus clouds extend as high as 13–18 km.

Distinguishing clouds from background aerosols in aerosol extinction retrievals is far from straightforward. The use of an averaged line of sight in retrieval methods for solar occultation measurements, the inhomogeneous nature of cloudiness, and the lack of coincident data available for comparisons make the distinction between clouds and aerosols very uncertain. Many approaches toward cloud identification from occultation and limb emission measurements have been attempted (e.g. Kent et al., 1997; Fromm et al., 1997; Nedoluha et al., 2003; von Savigny et al., 2005; Spang et al., 2005; Vanhellemont et al., 2005).

Recently, two major space occultation instruments have been put into orbit. The GOMOS spectrometer on board the European satellite ENVISAT is functioning since March 2002. It is a UV–Vis–NIR spectrometer aimed at the observation of stellar occultations from an heliosynchronous circular orbit at an altitude of 800 km (Kyrölä et al., 2004).

The Atmospheric Chemistry Experiment (ACE) (Bernath et al., 2005) was launched in August 2003 aboard the Canadian scientific satellite SCISAT-I. ACE circles the Earth at an altitude of 650 km with an orbital inclination of 74°. Solar occultation is the primary observation technique used by the onboard instruments, which consist of a high-resolution Fourier Transform Spectrometer (ACE-FTS), a dual optical spectrophotometer (MAESTRO), and two filtered imagers, operating in the Visible and NIR.

In this paper, we present an intercomparison between ACE and GOMOS aerosol extinction and cloud data. PSCs as well as cirrus clouds are observed by both instruments. After a brief description of the instruments, aerosol extinction and cloud characteristics are compared for the years 2004 and 2005. Finally, a synergistic use of both data sets proves their compatibility.

2. GOMOS measurements

GOMOS (Global Ozone Monitoring by Occultation of Stars) is a UV/Vis/NIR spectrometer that works in occultation mode: while orbiting the Earth, the instrument measures the transmission of light from stars that are setting below the Earth's horizon. Since the starlight has to pass through the Earth's atmosphere, it is partly scattered and/or absorbed by atmospheric gases and particles. During one orbit, 20–40 occultations are measured. In this way, several hundreds of occultations can be measured per day, allowing a good global coverage. Measurements are taken both on the dark and Sun-illuminated side of the Earth. For day side observations, the measurements are corrected by subtracting the bright limb component, that is measured with the upper and lower bands of the CCD detector. Nevertheless, after subtraction, the residual noise is large enough to significantly decrease the retrieval accuracy. Also, the UV spectrometer is saturated by the limb scattered light below 30 km. We therefore decided to use only dark-side measurements. After this data selection, 91,482 occultations were left to use (Fig. 1).

The spectrum of the starlight is measured by four spectrometers operating in a wavelength range from 250 to 950 nm. Additionally, GOMOS is equipped with two fast photometers of which the signals are used to correct for star scintillation and to retrieve high-resolution temperature profiles. Typically, the UV/Vis range combined with the sensitivity of the GOMOS spectrometers allows the retrieval of ozone, NO_2 , air, NO_3 , O_2 and aerosol extinction profiles (Kyrölä et al., 1993). While ozone can be retrieved up to 100 km of altitude, the other species are usually only detectable from the upper troposphere to about 50 km.

Unlike the case for gases, where the extinction cross sections are known from laboratory measurements, the aerosol extinction spectrum is *a priori* unknown. Typically, some parametrized function of wavelength is used. Vanhellemont et al. (2006) suggest the use of a quadratic polynomial of wavelength for GOMOS data, since this form can adequately approximate flat spectra (large particles), steep spectra (small particles), spectra with a maximum in the visible, etc.

3. ACE measurements

The Atmospheric Chemistry Experiment (ACE) was launched in August 2003 onboard the Canadian scientific satellite SCISAT-I, and is at present fully operational. The main instrument on board is a high-resolution (0.02 cm^{-1}) Fourier Transform Spectrometer (FTS) operating from 750 to 4400 cm^{-1} . During sunrise and sunset, the FTS measures infrared absorption signals to provide vertical profiles of atmospheric constituents (gases and particles). Aerosols and clouds can also be monitored by using the extinction of solar radiation as measured by two filtered imagers. The VIS filter is centered at 527 nm and has a

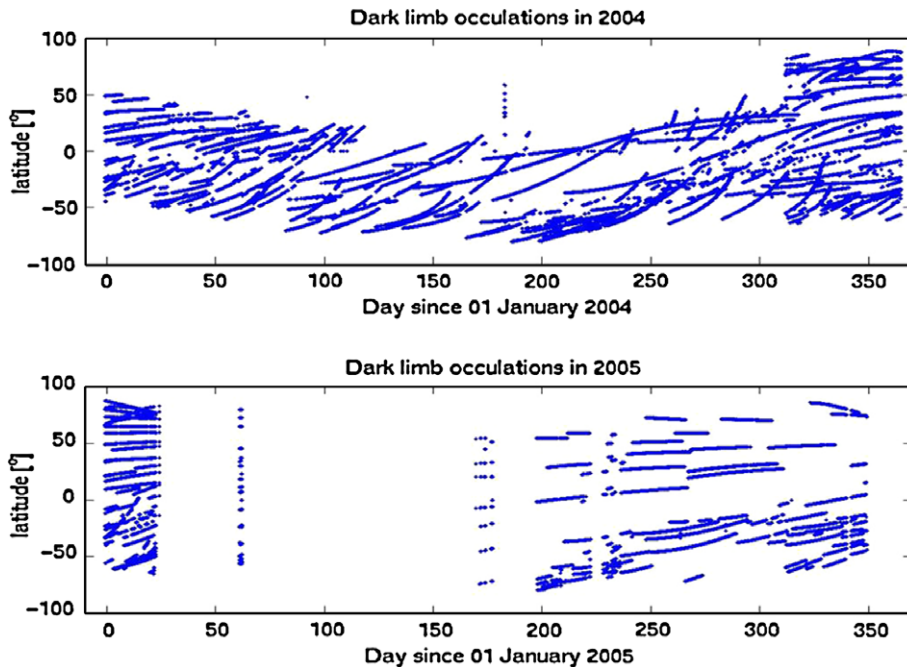


Fig. 1. GOMOS dark limb occultations for the years 2004 and 2005.

bandwidth (full width at half the maximum transmission) of 13 nm. The NIR filter is centered at 1020 nm with a FWHM bandwidth of 19 nm. After binning, the imager signals consist of 128×128 active pixel sensors. The total field of view (FOV) of the imagers is 30 mrad, to be compared to the 9 mrad angular diameter of the Sun. The satellite operates from a circular orbit at an altitude of 650 km, and the orbital plane inclination of 74° allows a global coverage with some predominance of the polar regions (Fig. 2).

Unfortunately, both imagers were left with some major handicaps of which the effect of the shifting multiple images on the pixels intensities is the biggest unknown. Despite these problems, the signal-to-noise ratio for the imagers is very good: 1500 for an image pixel at the center of the unrefracted Sun.

Transmittances are calculated only for the pixels deemed to be in the center of the ACE-FTS FOV (i.e. the center of the Sun), as determined from the pre-launch registration measurements, and post-launch checks of the registration. The results are averaged for three adjacent pixels to improve the signal-to-noise ratio. The three pixels are within the FTS FOV and are from the same row of the image (and thus have the same tangent altitude). Tangent heights are assigned to the transmittance data through the time stamps of the ACE-FTS and imager measurements, with an accuracy of about 1 km. We refer to Boone et al. (2005) for a detailed description of ACE-FTS retrievals and to Gilbert et al. (2007) for imager retrievals. From the transmittance data, a profile for total atmospheric extinction at both wavelengths was retrieved by using a vertical inversion algorithm.

Aerosol extinction profiles were obtained by subtracting the gas extinction contributions (air, O₃, NO₂), derived from the FTS measurements, from the total atmospheric extinction profiles. Since the used imager pixels are within the LOS of the FTS, our approach is reasonable.

Gilbert et al. (2007) also performed a preliminary validation of ACE imager slant path profiles of optical depth. On average, the ACE VIS imager gives results that are 5% lower than SAGE II, and the NIR imager 20% higher.

4. Cloud detection

Historically, UTLS cloud detection using occultation measurements has been performed in a variety of ways. McCormick et al. (1982) observed, in SAM profiles, layers of aerosol extinction considerably greater than background reference conditions and called these PSCs. They used a PSC extinction threshold of $8 \times 10^{-4} \text{ km}^{-1}$. Woodbury and McCormick (1986) used a fixed value of SAGE II extinction at 1.02 μm as a cloud threshold for cirrus. McCormick et al. (1989) used a 1 μm extinction ratio (SAM/Rayleigh) to identify PSCs. Pitts et al. (1990) used Arctic SAGE II aerosol extinction profiles to describe a PSC event in January and February 1989, employing an aerosol extinction ratio (using 525 and 1020 nm channels) in addition to enhancements in 1020 nm extinction to distinguish PSCs from background reference conditions. SAGE II 1020 nm extinctions were also used by Yue et al. (1994) to detect and analyze an unusual boreal summertime stratospheric cloud event in 1990. Here, the extinction enhancement in several altitude bins well above the tropopause was revealed by comparison with precloud

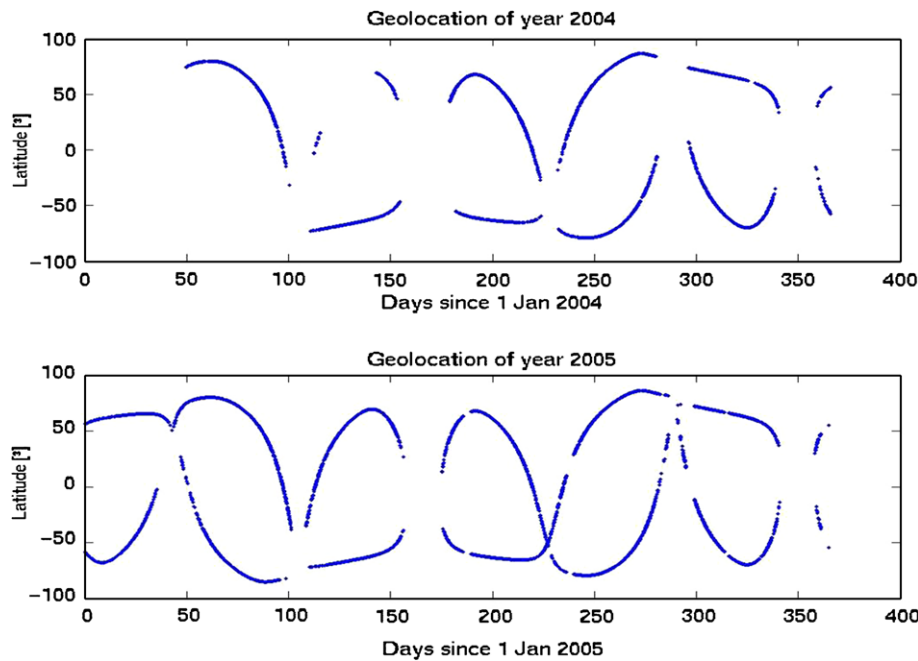


Fig. 2. ACE occultations for the years 2004 and 2005.

event extinctions and extinctions from the same period in the prior year.

In addition to enhanced aerosol layers, there is another manifestation of stratospheric cloudiness in retrieved altitude profiles. Under sufficiently cloudy conditions each instrument experiences an abnormally high profile termination altitude. This artifact common to the solar and stellar occultation methods of limb remote sounding (in this paper referred to as ‘high-Zmin’) has been exploited as a tropospheric and stratospheric cloud predictor (Wang et al., 1995a). As with aerosol enhancements, the high-Zmin conditions were described by the above authors in reference to standard profile termination altitudes.

Two manifestations of PSCs and cirrus clouds in GOMOS and ACE aerosol extinction profiles are considered in our cloud detection method: (1) a layer of enhanced extinction and (2) termination or commencement of the occultation event at an anomalously high tangent altitude.

In addition, ACE 2D imager data are useful to detect clouds. Dodion et al. (2007) discovered significant differences between PSCs and cirrus clouds exploring 2D imager data. PSCs appear as ‘symmetric’ layers, no horizontal or vertical ‘structure’ is detected within the PSC, suggesting that PSCs are uniform clouds with a very large horizontal extent. On the other hand, cirrus cloud image geometry is not well-defined. Also, cirrus clouds seem to have typical horizontal dimensions of about 20–30 km (Figs. 3 and 4).

5. Analysis of the years 2004 and 2005

Besides an intercomparison of aerosol extinction, we investigate in the following sections the temporal and lati-

tudinal variation of the derived PSC altitudes and the latitudinal variation of the observed tropical cirrus clouds.

5.1. Aerosol extinction intercomparison

In this section, we present UTLS aerosol zonal median values derived by GOMOS and ACE. Such values serve many purposes. In a qualitative way, a global picture of aerosols and clouds gives insight into the reasons for the variability of these species. Furthermore, zonal median values can be used in other studies that need a quantitative characterization of aerosols and clouds, such as UTLS chemistry modeling, optical calculations and remote sensing measurement corrections.

The spatial grid that we use consists of 18 latitude bins with a width of 10°, with bin centers ranging from 85°S to 85°N. The altitude grid consists of bins having a width of 1 km from 0 to 80 km. No variations along longitude are considered. We furthermore use monthly bins, from January 2004 until December 2005.

Every bin contains a number of data points, of which the statistical distribution is a priori unknown. It is expected that such distribution is asymmetric, with strong outliers. In such cases, the statistical mean is a poor way to describe the central tendency of the distribution. Therefore, the use of the median was our preferred estimator.

Figs. 5 and 6 show yearly zonal median aerosol extinction values. Clearly visible is the umbrella-shaped aerosol layer, having the largest altitudes above the equator and gradually sloping downwards in the direction of the poles. An interesting feature is the isolated maximum in the tropics at an altitude of 15–17 km measured by GOMOS, revealing the presence of high subvisual tropical cirrus

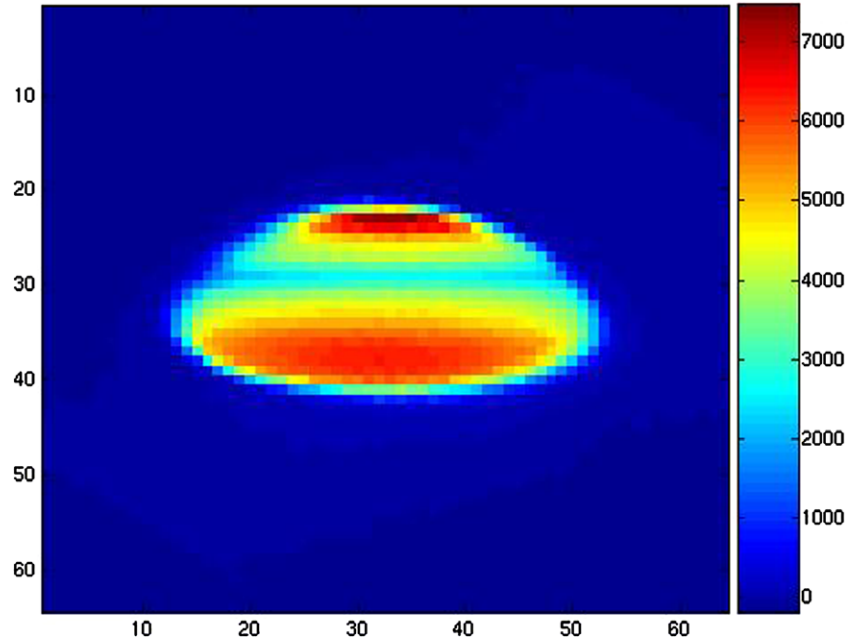


Fig. 3. Imager data at 1.020 μm revealing a PSC layer, July 9, 2004 at lat = 61°S. Since this is raw imager data, note that vertical and horizontal scale is pixels. One pixel has a horizontal and vertical dimension of 0.7 km at the tangent point.

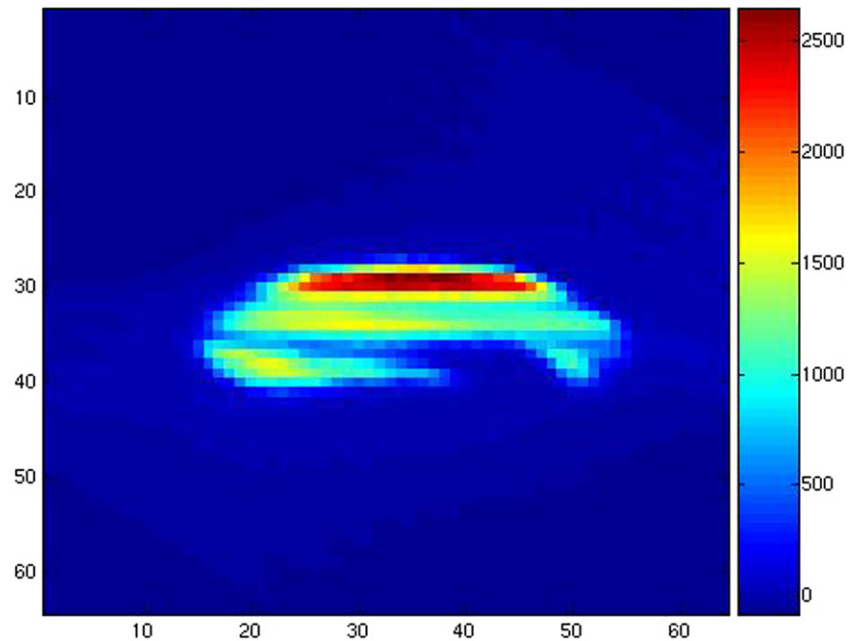


Fig. 4. Imager data at 1.020 μm revealing a cirrus cloud, February 20, 2005 at lat = 5°N.

clouds. ACE yearly zonal median aerosol extinction plots show a similar feature, however the maximum is not isolated with respect to altitude. Most probably, this difference between GOMOS and ACE data is caused by the large difference of SNR. As mentioned before, a well-known artifact of solar and stellar occultation methods is the high-Zmin condition. Since GOMOS has to deal with a very weak signal (stars) compared to ACE (Sun), this high-Zmin condition is much more expected. The absence of tropical cirrus clouds beneath 15 km in GOMOS yearly

aerosol extinction data is probably caused by termination of the cirrus contaminated occultations at an anomalously high tangent altitude.

The elevated extinction levels in the Arctic and Antarctic regions are most certainly caused by the occurrence of PSCs in the Arctic and Antarctic vortex. The much lower occurrence of Arctic PSCs, due to the weaker polar vortex, explains the less prominent Arctic feature. Since ACE was not yet operational in the winter of 2004, the difference between the upper and lower panel in Fig. 6 is expected.

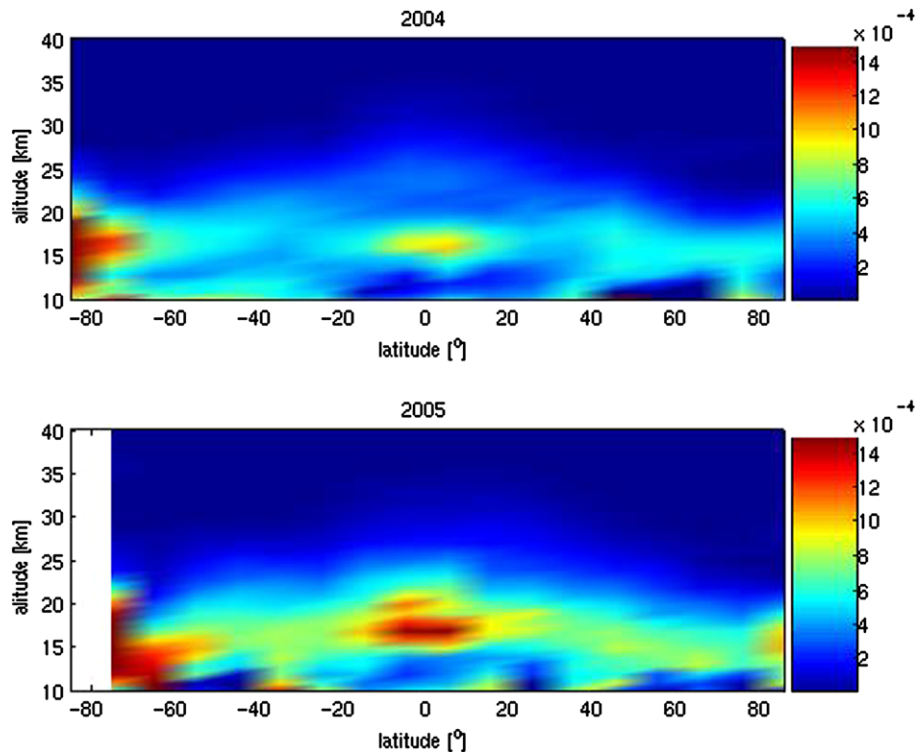


Fig. 5. GOMOS yearly zonal median aerosol extinction [km^{-1}]. Color scale is limited between 0 and $1.5 \times 10^{-3} \text{ km}^{-1}$ for all the median aerosol extinction plots.

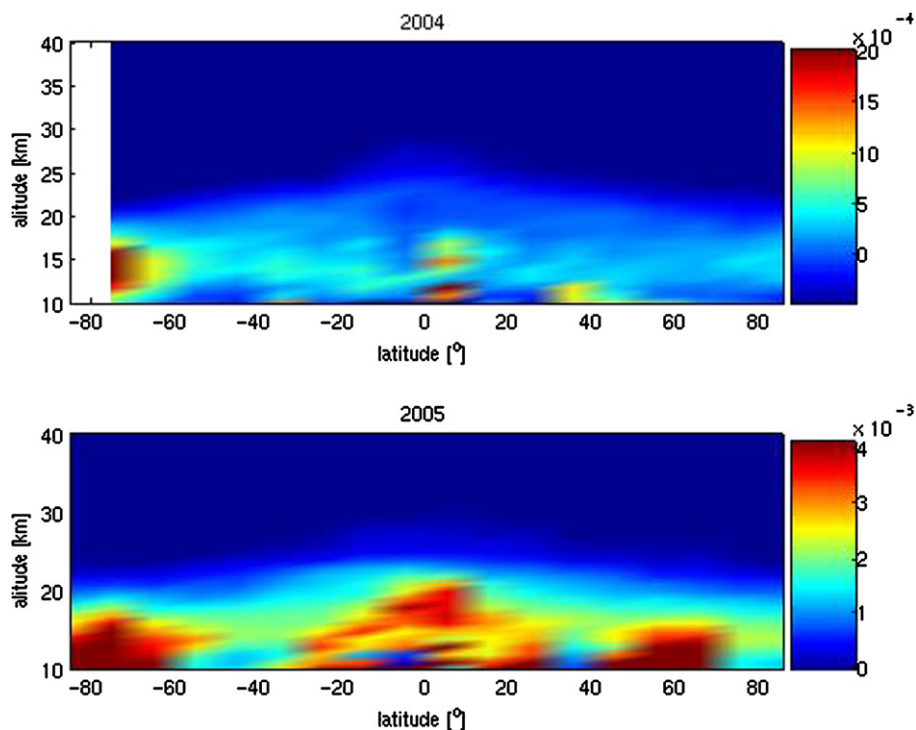


Fig. 6. ACE yearly zonal median aerosol extinction [km^{-1}].

Finally, a significant elevation of the overall aerosol extinction layer in 2005 compared to 2004 is clearly visible for

GOMOS as well as ACE data. The reason is not clear and, as far as we know, this is never reported before.

Figs. 7–10 show four plots of ACE and GOMOS zonal median aerosol extinction, averaged for 3-month periods. Because of the formation of PSCs, July, August and September are characterized by enhanced aerosol extinction at latitudes polewards of 50°S. Although not very clear, northern PSCs showing up in winter cause a similar feature northwards of 50°N. The last panel of Fig. 8 is a good example. Finally, the cirrus cloud feature, mentioned before, gradually moves toward the North, and then heads back southwards at the end of the year. A more detailed analysis of this well-known seasonal variation of cirrus cloud occurrence is investigated in Section 5.3.

5.2. Temporal evolution of Southern Hemisphere PSC altitude

SH PSCs are frequently detected by GOMOS and ACE. Figs. 11 and 12 show median aerosol extinction profiles of selected PSCs. Clearly visible is the PSC signature at altitudes around 15 km.

By “PSC altitude” we mean the tangent height for which the cloud signature reaches its maximum aerosol extinction value. We clearly see a descent of PSCs as time progresses. This slow descent of PSCs has also been reported in other studies. Santacesaria et al. (2001) discuss three possible reasons for the PSC descent. First, the sedimentation of the PSC particles, which can be excluded as an explanation for the apparent descent, since the sedimentation speeds are too large. Secondly, the slow diabatic descent of the

HNO_3 and H_2O distributions. This process leads to descent rates of less than 0.5 km/month, and is therefore not strong enough to solely cause the observed descent. Thirdly, the descent of the lower stratospheric temperature minimum. von Savigny et al. (2005) concluded from the very good agreement of descent rates of the temperature minimum and the PSC descent rates derived in his study that the temporal variation of the lower stratospheric temperature structure is the main driver of the PSC descent.

Table 1 contains the SH PSC descent rates derived from our measurements for 2004 and 2005. We obtain more or less the same values for ACE and GOMOS. On average, the observed descent rates are 2.3 km/month for the 50°S–60°S latitude band, 1.9 km/month for the 60°S–70°S latitude band and 0.7 km/month for latitudes between 70°S and 80°S. These results are in very good agreement with the SCIAMACHY measurements by von Savigny et al. (2005) and the LIDAR measurements by Santacesaria et al. (2001). Vanhellemont et al. (2005) already presented aerosol extinction measurements with GOMOS. Although no PSC descent rates were derived, the observed PSC descent is in good agreement with the results presented here.

5.3. Latitudinal variation of tropical cirrus clouds

By grouping the 2-year ACE and GOMOS data, the seasonal variations of tropical cirrus cloud occurrence may be examined. As shown in Fig. 13, the tropical maximum in GOMOS aerosol extinction moves from about 5°S in win-

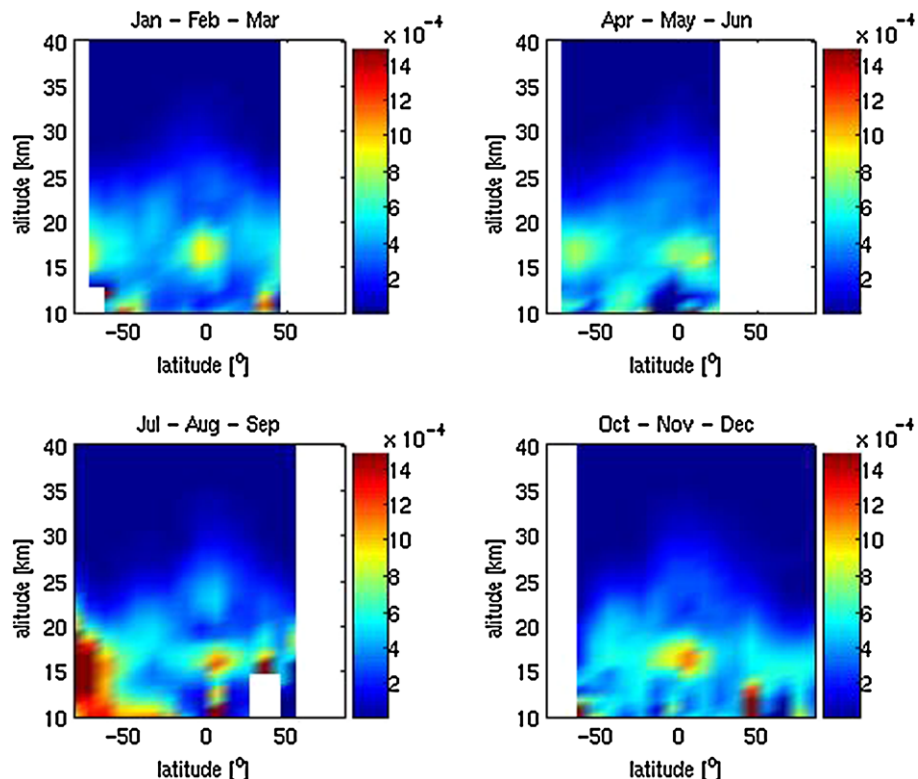
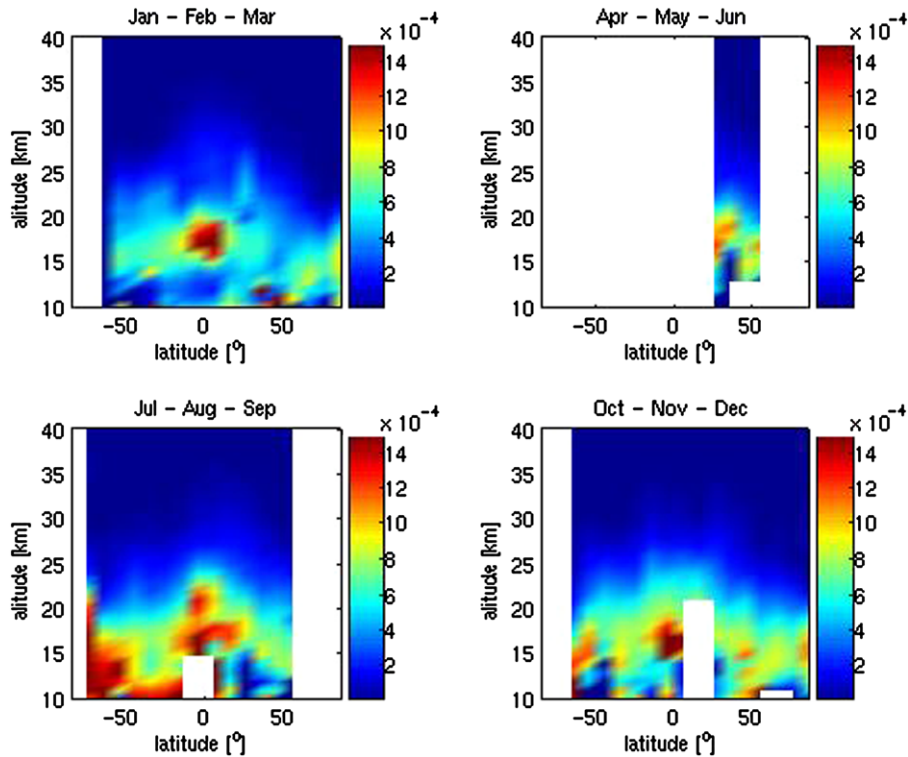
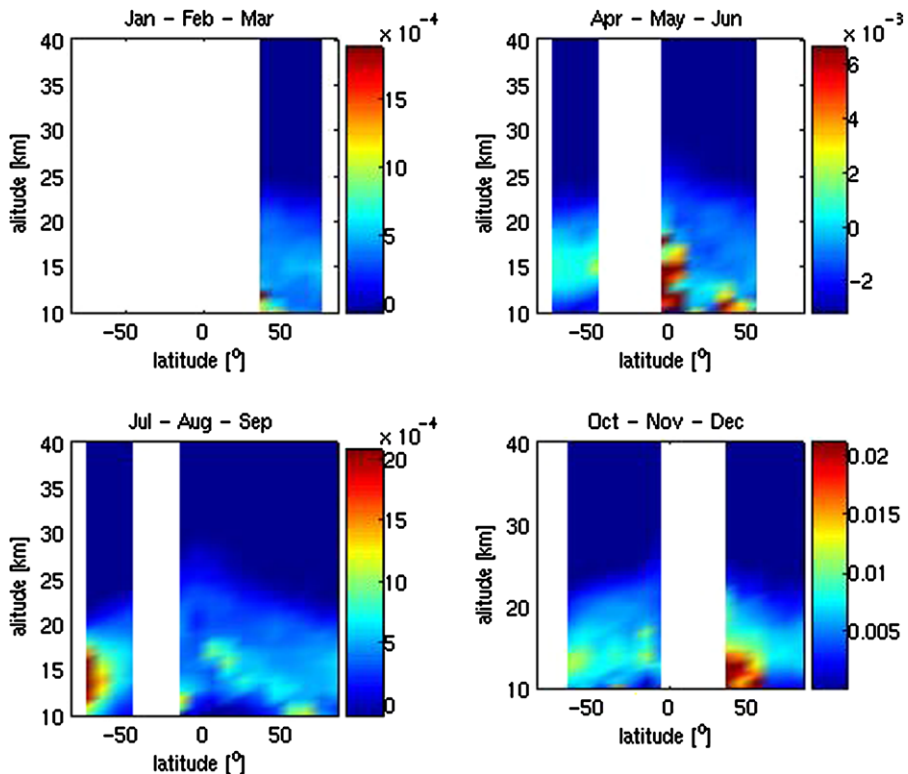


Fig. 7. GOMOS seasonal zonal median aerosol extinction of 2004 [km^{-1}].

Fig. 8. GOMOS seasonal zonal median aerosol extinction of 2005 [km^{-1}].Fig. 9. ACE seasonal zonal median aerosol extinction of 2004 [km^{-1}].

ter and spring to about 5°N in summer and fall. The same latitudinal movement for ACE cirrus clouds is observed, however a lack of winter and fall data hampers general

conclusions. This well-known latitudinal variation of tropical cirrus clouds has been reported before (e.g. Rossow and Lacis, 1990; Wang et al., 1996) and is correlated with

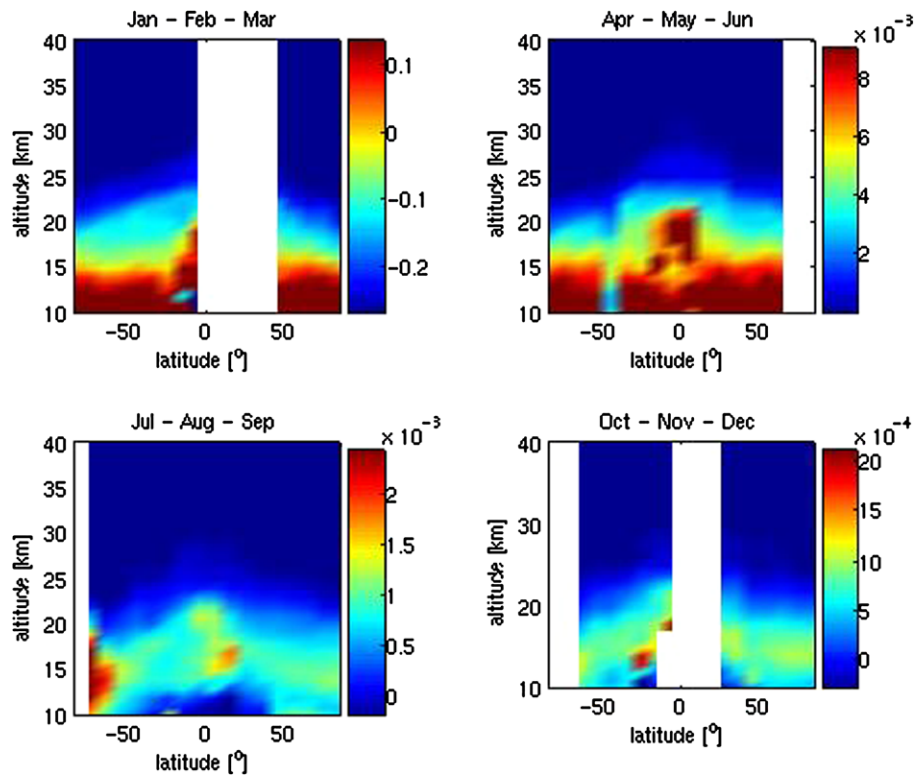


Fig. 10. ACE seasonal zonal median aerosol extinction of 2005 [km^{-1}].

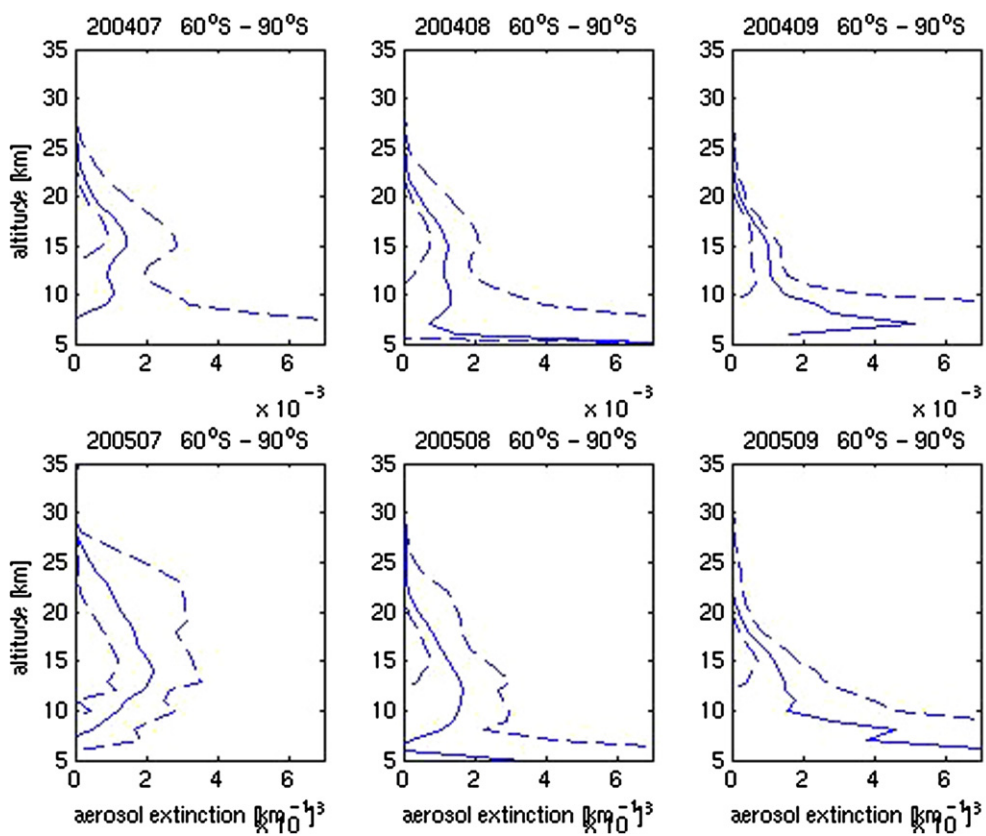


Fig. 11. GOMOS median aerosol extinction profiles of the selected SH PSCs. Dashed lines represent the 16 and 84 percentiles.

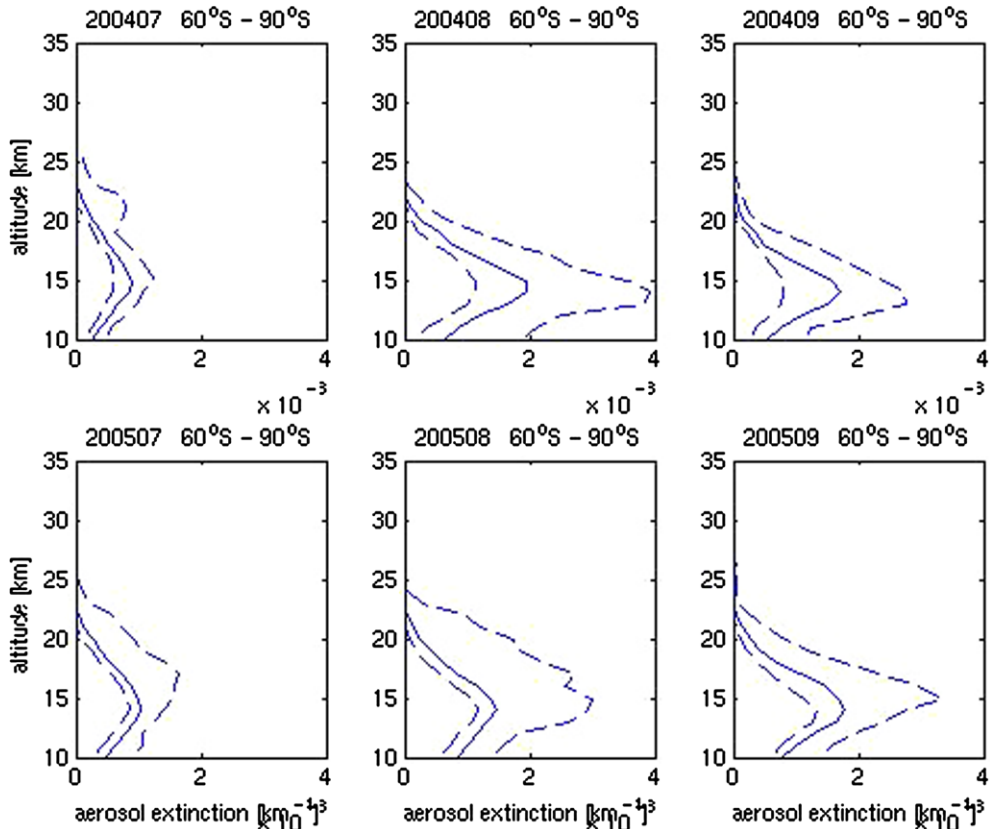


Fig. 12. ACE median aerosol extinction profiles of the selected SH PSCs. Dashed lines represent the 16 and 84 percentiles.

Table 1
Mean PSC descent rates [km/month] for ACE and GOMOS in the Southern polar vortices of 2004 and 2005

	2004 GOMOS	2004 ACE	2005 GOMOS	2005 ACE
70°–80°	0.4	0.8	0.9	0.5
60°–70°	2.0	1.6	2.1	1.8
50°–60°	2.3	2.2	2.5	2.5

the seasonal shift of the Intertropical Convergence Zone (ITCS).

6. Synergetic use of GOMOS and ACE imager data

Although both experiments are using the limb occultation technique, they considerably differ in many aspects of which the following two are the most important: (1) stars are faint light sources of variable magnitude and temperature that hardly compete with the very large constant SNR delivered by the Sun; (2) the stellar occultations can be observed at a higher rate (20–40 per orbit) instead of the unique sunrise/sunset pair per orbit. Usually, as shown above, cloud signatures are detected on aerosol extinction profiles. However, Dodion et al. (2007) proved the ability of ACE 2D imager data to be an efficient cloud detector in the UTLS region. Moreover, the nature and structure of PSCs and cirrus clouds could be derived. So, the excellent global coverage of GOMOS

in synergetic use with the 2D ACE imager data promises to reveal global cloud occurrence, nature and characteristics in both a quantitative and qualitative way. Since this work is still in a preliminary phase, we only show one coincident measurement of a double layered PSC (Figs. 14 and 15).

7. Conclusions

The presented zonal median aerosol extinction values constructed from the night-time subset of the entire 2004 and 2005 GOMOS data set has been able to provide quality aerosol extinction profiles. All the features that ought to be expected are detected: the typical shape of the aerosol layer, the occurrence of PSCs within the Antarctic and Arctic winter vortex and the occurrence of tropical subvisual cirrus clouds. Preliminary ACE imager data, dealing with a rather limited global coverage compared to GOMOS, provide similar median aerosol extinction plots. However, the latitudinal variation of tropical cirrus clouds could not be extracted due to gaps in the data. A significant elevation of the overall aerosol extinction layer in 2005 compared to 2004 is clearly visible for GOMOS as well as ACE data.

In addition, individual profiles provide a lot of information about cloud nature and characteristics. Two manifestations of PSCs and cirrus clouds in GOMOS and

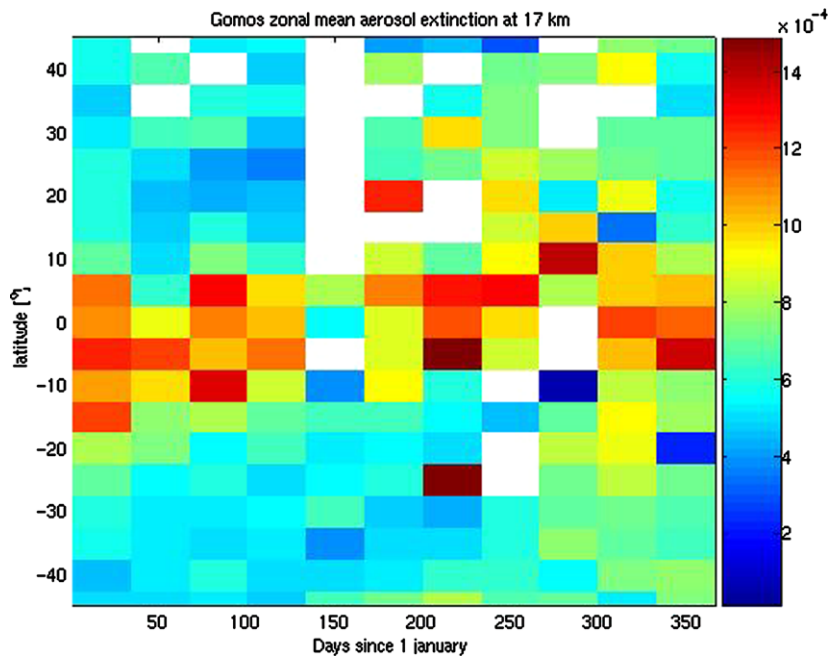


Fig. 13. Two-year zonal median time/latitude plot of GOMOS tropical aerosol extinction data at 17 km altitude.

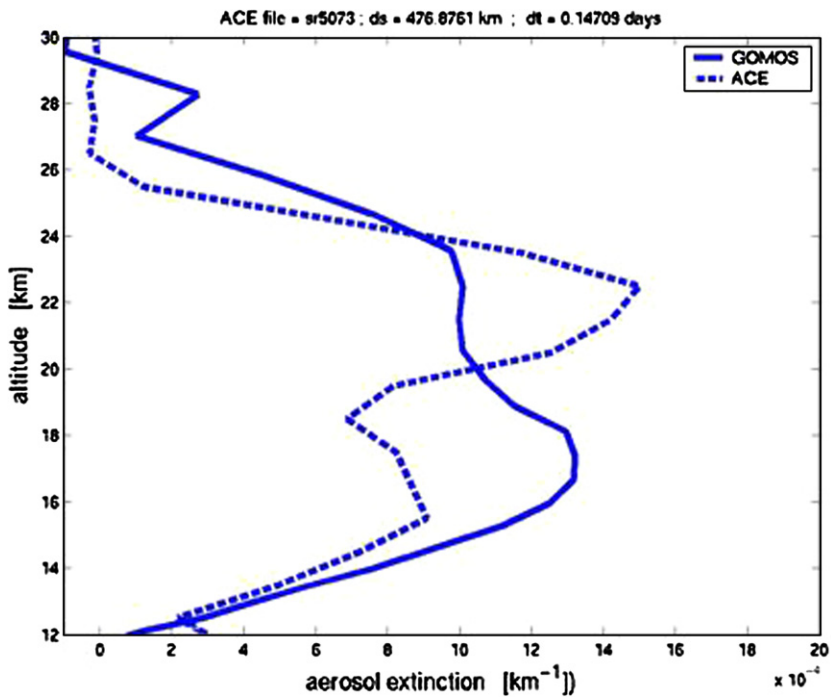


Fig. 14. Aerosol extinction profiles of GOMOS and ACE, both revealing the presence of a the same double layered PSC.

ACE aerosol extinction profiles are exploited in the cloud detection method: (1) a layer of enhanced extinction and (2) termination or commencement of the occultation event at an anomalously high tangent altitude. In addition, ACE 2D imager data is useful to detect clouds. The temporal and latitudinal variation of PSCs in the Antarctic vortex was investigated. Derived descent rates

are in good agreement with each other and with values obtained from literature.

Finally, the excellent global coverage of GOMOS in synergistic use with the aerosol extinction and 2D raw ACE imager data promises to reveal global cloud occurrence, nature and characteristics in both a quantitative and qualitative way.

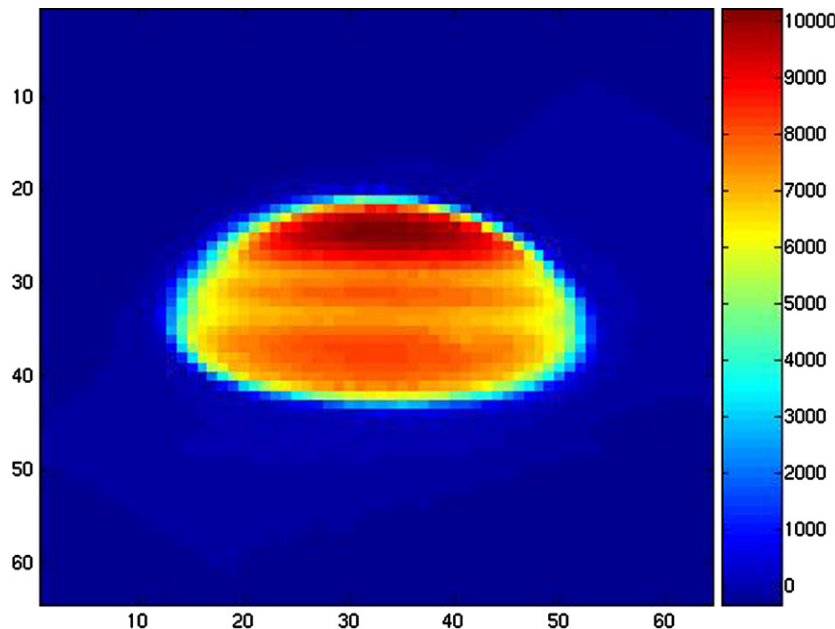


Fig. 15. Raw imager data of the coincident double layered PSC measurement.

Acknowledgements

The present study was funded by the PRODEX 7 contract SADE under the authority of the Belgian Space Science Office (BELSPO). The ACE mission is funded by the Canadian Space Agency and the Natural Sciences and Engineering Research Council of Canada (NSERC). Funding at Waterloo is also provided by the NSERC-Boomer-MSC Industrial Research Chair in Fourier Transform Spectroscopy.

References

- Bernath, P.F., McElroy, C.T., Abrams, M.C., Boone, C.D., Butler, M., Camy-Peyret, C., Carleer, M., Clerbaux, C., Coheur, P.-F., Colin, R., De Cola, P., De Mazière, M., Drummond, J.R., Dufour, G., Evans, W.F.J., Fast, H., Fussen, D., McConnell, J.C., McHugh, M., McLeod, S.D., Michaud, R., Midwinter, C., Nassar, R., Nichitiu, F., Nowlan, C., Rinsland, C.P., Rochon, Y.J., Rowlands, N., Semeniuk, K., Simon, P., Skelton, R., Sloan, J.J., Soucy, M.-A., Strong, K., Tremblay, P., Turnbull, D., Walker, K.A., Walker, I., Wardle, D.A., Wehrle, V., Zander, R., Zou, J. Atmospheric Chemistry Experiment (ACE): mission overview. *Geophys. Res. Lett.* 32, L15S01, doi:10.1029/2005GL022386, 2005.
- Boone, Chris D., Nassar, Ray, Walker, Kaley A., Rochon, Yves, McLeod, Sean D., Rinsland, Curtis P., Bernath, Peter F. Retrievals for the atmospheric chemistry experiment Fourier-transform spectrometer. *Appl. Opt.* 44 (33), 7218–7231, 2005.
- Dodion, J., Fussen, D., Vanhellemont, F., Bingen, C., Mateshvili, N., Gilbert, K., Skelton, R., Turnbull, D., McLeod, S.D., Boon, C.D., Walker, K.A., Bernath, P.F., Cloud detection in the upper troposphere – lower stratosphere region via ACE imagers: a qualitative study. *J. Geophys. Res.* 112, in press, doi:10.1029/2006JD007160, 2007.
- Dutton, E., Christy, J. Solar radiative forcing at selected locations and evidence for global lower tropospheric cooling following the eruptions of El Chicón and Pinatubo. *Geophys. Res. Lett.* 19, 2313–2316, 1992.
- Farman, J.C., Gardiner, B.G., Shanklin, J.D. Large losses of Total Ozone in Antarctica Reveal Seasonal ClO_x/NO_x Interaction. *Nature* 315, 207–210, 1985.
- Fromm, M.D., Bevilacqua, R.M., Lumpe, J.D., Shettle, E.P., Hornstein, J.S., Massie, S.T., Fricke, K.-H. Observations of Antarctic polar stratospheric clouds by POAM II: 1994–1996. *J. Geophys. Res.* 102 (D19), 23659–23672, doi:10.1029/97JD00794, 1997.
- Gilbert, K.L., Turnbull, D.N., Walker, K.A., Boone, C.D., McLeod, S.D., Butler, M., Skelton, R., Bernath, P.F., Chateauneuf, F., Soucy, M.-A. The On-Board Imagers for the Canadian ACE SCISAT-I Mission. *J. Geophys. Res.* 112, in press, doi:10.1029/2006JD007714, 2007.
- Jensen, E.J., Toon, O.B., Westphal, D.L., Kinne, S., Heymsfield, A.J. Microphysical modeling of cirrus 1. Comparison with 1986 FIRE IFO measurements. *J. Geophys. Res.* 99, 10421–10442, 1994.
- Junge, C., Chagnon, C., Manson, J. Stratospheric aerosols. *J. Meteor.* 18, 80–108, 1961.
- Kent, G.S., Wang, P.-H., Skeens, K.M. Discrimination of cloud and aerosol in the Stratospheric Aerosol and Gas Experiment III occultation data. *Appl. Opt.* 36 (33), 8639–8649, 1997.
- Kyrölä, E., Sihvola, E., Kotivuori, Y., Tikka, M., Tuomi, T., Haario, H. Inverse theory for occultation measurements. 1. Spectral Inversion. *J. Geophys. Res.* 98, 7367–7381, 1993.
- Kyrölä, E., Tamminen, J., Leppelmeier, G., Sofieva, V., Hassinen, S., Beraux, J., Hauchecorne, A., Dalaudier, F., Cot, C., Korablev, O., Fanton d'Andon, O., Barrot, G., Mangin, A., Théodore, B., Guirlet, M., Etanchaud, F., Snoeij, P., Koopman, R., Saveedra, L., Fraisse, R., Fussen, D., Vanhellemont, F. GOMOS on ENVISAT: an overview. *Adv. Space Res.* 33, 1020–1028, 2004.
- Liu, H.-L., Wang, P.K., Schlesinger, R.E. A numerical study of cirrus clouds. Part I: Model description. *J. Atmos. Sci.* 60 (8), 1075–1084, 2003a.
- Liu, H.-L., Wang, P.K., Schlesinger, R.E. A numerical study of cirrus clouds. Part II: Effects of Ambient Temperature, Stability, Radiation, Ice Microphysics, and Microdynamics on Cirrus Evolution. *J. Atmos. Sci.* 60 (9), 1097–1119, 2003b.
- McCormick, M.P., Steel, H.M., Hamill, P., Chu, W.P., Swissler, T.J. Polar stratospheric cloud sightings by SAM II. *J. Atmos. Sci.* 39, 1387–1397, 1982.
- McCormick, M.P., Trepte, C.R., Pitts, M.C. Persistence of polar stratospheric clouds in the southern polar region. *J. Geophys. Res.* 94, 11241–11251, 1989.

- Molina, M.J., Tso, T.L., Molina, L.T., Wang, F.C.-Y. Antarctic stratospheric chemistry of chlorine nitrate, hydrogen chloride and ice: release of active chlorine. *Science* 238, 1253–1257, 1987.
- Nedoluha, G.E., Bevilacqua, R.M., Fromm, M.D., Hoppel, K.W., Allen, D.R. POAM measurements of PSCs and water vapor in the 2002 Antarctic vortex. *Geophys. Res. Lett.* 30 (15), 1796, doi:10.1029/2003GL017577, 2003.
- Pitts, M.C., Poole, L.R., McCormick, M.P. SAGE II observations of polar stratospheric clouds near 50°N, January 31–February 2, 1989. *Geophys. Res. Lett.* 17, 405–408, 1990.
- Ramaswamy, V., Ramanathan, V. Solar absorption of cirrus clouds and the maintenance of the tropical upper troposphere thermal structure. *J. Atmos. Sci.* 46, 2293–2310, 1989.
- Randall, D.A., Harshvardan, Dazlich, D.A., Corsetti, T.G. Interactions among radiation, convection, and large-scale dynamics in a general circulation model. *J. Atmos. Sci.* 46, 1943–1970, 1989.
- Rossow, W.B., Lacis, A.A. Global, seasonal cloud variations from satellite radiance measurements. Part II: Cloud properties and radiative effects. *J. Climate* 3, 1204–1253, 1990.
- Santacesaria, V., MacKenzie, A.R., Stefanutti, L. A climatological study of polar stratospheric clouds (1989–1997) from LIDAR measurements over Dumont d'Urville (Antarctica). *Tellus* 53B, 306–321, 2001.
- Solomon, S. Stratospheric ozone depletion: a review of concepts and history. *Rev. Geophys.* 37, 275–316, 1999.
- Spang, R., Remedios, J.J., Kramer, L.J., Poole, L.R., Fromm, M.D., Müller, M., Baumgarten, G., Konopka, P. Polar stratospheric cloud observations by MIPAS on ENVISAT: detection method, validation and analysis of the northern hemisphere winter 2002–2003. *Atmos. Chem. Phys.* 5, 679–692, 2005.
- Vanhellemont, F., Fussen, D., Bingen, C., Kyrölä, E., Tamminen, J., Sofieva, V., Hassinen, S., Veronen, P., Seppälä, A., Bertaux, J.L., Hauchecorne, A., Dalaudier, F., Fanton d'Andon, O., Barrot, G., Mangin, A., Theodore, B., Guirlet, M., Renard, J.B., Fraisse, R., Snoeij, P., Koopman, R., Saavedra, L. A 2003 stratospheric aerosol extinction and PSC climatology from GOMOS measurements on Envisat. *Atmos. Chem. Phys.* 5, 2413–2417, 2005.
- Vanhellemont, F., Fussen, D., Dodion, J., Bingen, C., Mateshvili, N. Choosing a suitable analytical model for aerosol extinction spectra in the retrieval of UV/Visible satellite occultation measurements. *J. Geophys. Res.* 111, D23203, doi:10.1029/2005JD006941, 2006.
- von Savigny, C., Ulasi, E.P., Eichmann, K.-U., Bovensmann, H., Burrows, J.P. Detection and mapping of polar stratospheric clouds using limb scattering observations. *Atmos. Chem. Phys.* 5, 3071–3079, 2005.
- Wang, P.-H., McCormick, M.P., Minnis, P., Kent, G.S., Yue, G.K., Skeens, K.M. A method for estimating vertical distribution of the SAGE II opaque cloud frequency. *Geophys. Res. Lett.* 22, 243–246, 1995a.
- Wang, P.-H., Minnis, P., McCormick, M.P., Kengt, S.K., Skeens, K.M. A 6-year climatology of cloud occurrence frequency from Stratospheric Aerosol and Gas Experiment II observations (1985–1990). *J. Geophys. Res.* 101 (D23), 29407–29429, 1996.
- Woodbury, G.E., McCormick, M.P. Zonal and geographical distribution of cirrus clouds determined from SAGE data. *J. Geophys. Res.* 91, 2775–2785, 1986.
- Yue, G.K., Veiga, R.E., Wang, P.H. SAGE II observations of a previously unreported stratospheric volcanic cloud in the northern polar summer of 1990. *Geophys. Res. Lett.* 21, 429–432, 1994.